

Theoretical Study of the Low-Lying Electronically Excited States of Diacetylene

Fernando Vila, Piotr Borowski,* and Kenneth D. Jordan

Department of Chemistry and Center for Molecular and Materials Simulations, University of Pittsburgh, Pittsburgh, Pennsylvania 15260

Received: May 31, 2000

The complete-active-space SCF and CASMP2 methods are used to characterize the low-lying excited singlet and triplet states of diacetylene. With the exception of the $1^1\Delta_u$ state, all excited states considered are found to have geometrical structures distorted away from linear. Three of the triplet states are predicted to have non-planar C_2 -symmetry structures. The other states are predicted to be planar, existing as both cis (C_{2v}) and trans (C_{2h}) isomeric forms. Vibrational frequencies are calculated for the low-lying electronically excited states, and vertical and adiabatic excitation energies are reported.

Introduction

Diacetylene is an important species in hydrocarbon flames and in the atmosphere of Neptune and Titan.^{1–4} Recent experimental studies have addressed reactions between diacetylene, excited into low-lying triplet states, and other hydrocarbons.^{5–8} Interpretation of these experimental results has been hampered by the paucity of information on the triplet states of diacetylene. The most thorough theoretical study of the low-lying excited states of diacetylene is that of Karpfen and Lischka (KL).⁹ Although the KL study is a valuable starting point, the basis set and configuration lists used were quite small, and as a result, there could be sizable errors in the optimized structures and in the relative energies of the various states. Moreover, only a few states were considered, and those that were studied were assumed to have planar structures.

In the present study, the complete-active-space SCF (CAS-SCF^{10–12}) and multireference MP2 (CASPT2^{13–15}) methods have been employed together with flexible basis sets to characterize the low-lying triplet and singlet states of diacetylene. The CASPT2 method, in particular, allows for a more complete treatment of electron correlation effects than do the methods used in the KL study. Several electronic states not considered in the KL study are examined, and vibrational frequencies are calculated for the optimized structures to establish that they are true minima. The following sections of the paper give a brief background on the electronic structure of diacetylene, provide a description of the theoretical approaches used, and present and discuss the results of the calculations.

Background

Diacetylene in its ground electronic state has a linear ($D_{\infty h}$) geometrical structure and a $(1\pi_u)^4(1\pi_g)^4(2\pi_u^*)^0(1\sigma_u^*)^0(1\sigma_g^*)^0(2\pi_g^*)^0$ electronic configuration,⁹ where the occupied σ orbitals have been suppressed and the low-lying unfilled MO's have been indicated. Figure 1 reports the variation of the energies of the frontier orbitals of diacetylene with cis and trans bending. In generating these results, only the CCH angles were varied; the CC and CH bond lengths and the CCC angles were fixed at their ground state (CASSCF-level) values. Although those

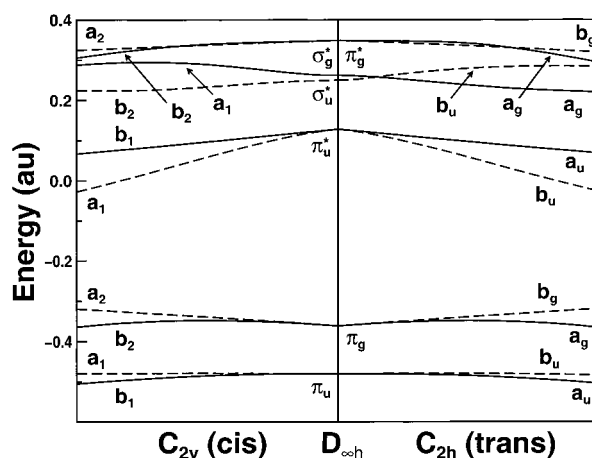


Figure 1. Energies of the frontier orbitals of diacetylene as a function of the CCH angle. The orbital energies were obtained from Hartree–Fock calculations using the 3-21G basis set.

excited states with bent equilibrium structures have CCC angles different from 180° , most of the energy lowering associated with the distortion from the linear structure is expected to be due to the CCH bending. Thus, the approach adopted here, in which only the CCH angles are varied, should suffice for providing a qualitative picture of how the energies of the various orbitals change with bending.

As seen from Figure 1, the two components of the π_u^* LUMO drop rapidly in energy upon either cis or trans CCH bending, with the in-plane component (which is of a_1 and b_u symmetry for the cis and trans distortions, respectively) being particularly strongly stabilized by the bending. In contrast, the energies of the π orbitals and the higher-lying π^* orbital are relatively insensitive to the bending of the CCH groups. The other important observation is that the splitting between the two occupied π orbitals is considerably smaller than that between the two π^* orbitals (at least for structures not too distorted from linear).

The low-lying electronically excited states for the linear molecule are expected to derive from HOMO \rightarrow LUMO ($1\pi_g \rightarrow 2\pi_u^*$) excitations, giving rise to Δ_u , Σ_u^+ and Σ_u^- states. On the basis of the orbital correlation diagram shown in Figure 1, all of these states are expected to be bent. The next set of valence

* Corresponding author. Present address: Department of Chemistry, Marie Curie Skłodowska University, 20-031 Lublin, Poland.

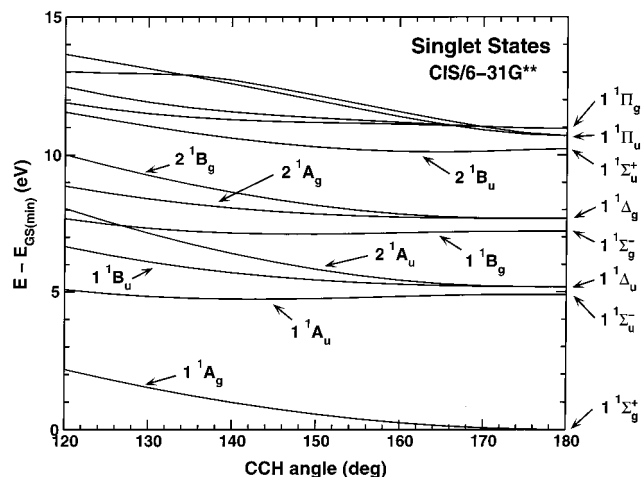


Figure 2. Variation of the energies of the low-lying singlet electronic states of diacetylene as a function of the CCH angle. Results are shown for trans bending only. The ground-state energies are from HF/6-31G** calculations, and the excited-state energies were obtained by combining CIS/6-31G** excitation energies with the HF/6-31G** energy of the ground state.

excited states are expected to be derived from the HOMO-1 \rightarrow LUMO ($1\pi_u \rightarrow 2\pi_u^*$) excitations, with significant admixture of HOMO \rightarrow LUMO + 1 ($1\pi_g \rightarrow 2\pi_g^*$) excitations. These states, which are of Δ_g , Σ_g^+ and Σ_g^- symmetry, would also be expected to be distorted from linear. The lowest energy valence-type Π_u and Π_g states, derived from $1\pi_g \rightarrow 1\sigma_u^*$, $1\pi_g \rightarrow 1\sigma_g^*$, $1\pi_u \rightarrow 1\sigma_u^*$ and $1\pi_u \rightarrow 1\sigma_g^*$ excitations, and the lowest lying Rydberg states would be expected to fall energetically close to the highest of the Δ_g , Σ_g^+ , and Σ_g^- states described above.

Computational Details

The main approaches used in this study are the CASSCF¹⁰⁻¹² and CASMP2¹³⁻¹⁵ methods. However, because of the large number of possible low-lying electronically excited states of diacetylene, survey calculations using the configuration interaction singles (CIS) method were first undertaken to aid in identifying the states to investigate further using CASSCF and CASMP2 calculations. Specifically, starting with the CASSCF/6-31G** optimized geometry of the ground state, CIS calculations were carried out for CCH angles ranging from 180 to 120°, while retaining C_{2h} symmetry. (Details on the CASSCF calculations are provided below.) The carbon framework was kept linear, and the CC and CH bond lengths were kept frozen at the ground-state values.

The potential energy curves obtained from CIS calculations using the 6-31G** basis set¹⁶⁻¹⁸ are shown in Figures 2 and 3. For the linear equilibrium structure of the ground state, the CIS calculations predict the three lowest energy triplet states, in terms of increasing energy, to be $^3\Sigma_u^+$, $^3\Delta_u$, and $^3\Sigma_u^-$, followed by $^3\Sigma_g^+$, $^3\Delta_g$, and $^3\Sigma_g^-$, and then by $^3\Pi_u$, and $^3\Pi_g$. In the singlet manifold, the CIS calculations predict low-lying $^1\Sigma_u^-$ and $^1\Delta_u$ states, followed by $^1\Sigma_g^-$ and $^1\Delta_g$ states about 2 eV higher in energy, and then by $^1\Sigma_u^+$, $^1\Pi_u$, and $^1\Pi_g$ states roughly another 3 eV higher in energy. The lowest energy excited valence-type $^1\Sigma_g^+$ state is predicted to lie about 12 eV above the ground state.

Although our primary interest is in valence excited states of diacetylene, it is important to consider the possibility of “intrusion” of low-lying Rydberg states and valence/Rydberg mixing especially since electron energy-loss spectra of diacetylene display structure due to Rydberg states at energies as low as 6.6 eV.¹⁹ With a compact basis set such as that (6-31G**)

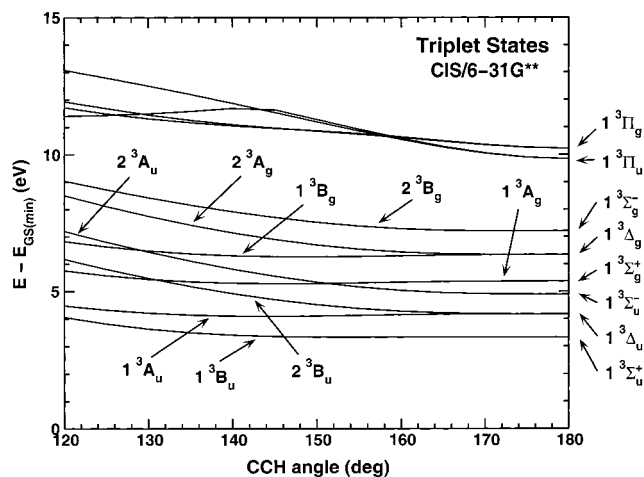


Figure 3. Variation of the energies of the low-lying triplet electronic states of diacetylene as a function of the CCH angle. Results are shown for trans bending only. The ground-state energies are from HF/6-31G** calculations, and the excited-state energies were obtained by combining CIS/6-31G** excitation energies with the HF/6-31G** energy of the ground state.

used for the CIS calculations described above, low-lying Rydberg states are “artificially” excluded, but with the more flexible ANO basis set,²⁰ which will be used in the CASSCF and CASMP2 calculations described below, this will not be the case.

At the equilibrium geometry of the ground electronic state, the lowest energy Rydberg states of diacetylene are expected to arise from $1\pi_g \rightarrow 3s$ and $1\pi_g \rightarrow 3p$ excitations, resulting in Π_g , Π_u , Σ_u^- , Δ_u , and Σ_u^+ states. CIS calculations with the ANO basis set predict the lowest energy Rydberg state to be of Π_g symmetry, as expected, and to fall near 7.2 eV, 0.6 eV above the energy at which it is observed experimentally. Examination of Figures 2 and 3 reveals that this places the lowest Rydberg states close in energy to the $1^3\Delta_g$, $1^3\Sigma_g^-$, $1^1\Sigma_g^-$, and $1^1\Delta_g$ states. These results will dictate how many valence states are included in the CASSCF and CASPT2 calculations.

For accurately describing electronically excited states of molecules it is essential to recover a significant fraction of the electron correlation. In this study this was accomplished by use of the CASSCF and CASMP2 methods. The active space for the CASSCF calculations was chosen to consist of the eight valence π and π^* molecular orbitals.

All possible symmetry- and spin-allowed arrangements of eight electrons in this eight orbital space were included, leading to the so-called CAS(8,8) method. This approach was used in conjunction with the 6-31G** basis set to optimize the geometries of the ground state and the low-lying excited states. The geometry of the ground state of diacetylene was optimized under the constraint of $D_{\infty h}$ symmetry. The excited states were optimized starting with cis and trans bent structures, i.e., in C_{2h} and C_{2v} symmetry, respectively. Vibrational frequencies were calculated in the harmonic approximation for each optimized structure. In those cases that the calculations gave an imaginary frequency, the geometry was reoptimized in lower symmetry, allowing for the distortion indicated by the eigenvector associated with the imaginary frequency. The frequencies were then calculated for the lower-symmetry structure to confirm that it is indeed a local potential energy minimum.

In the triplet manifold the eight lowest energy valence states (those derived from the $1^3\Sigma_u^+$, $1^3\Delta_u$, $1^3\Sigma_u^-$, $1^3\Sigma_g^+$, $1^3\Delta_g$, and $1^3\Sigma_g^-$ states of the linear molecule) were considered. In the singlet manifold six excited valence states (those derived from

TABLE 1: Optimized Geometries for the Low-Lying Electronic States of Diacetylene^a

state	method	basis set	r_{CH}	r_{CCo}	r_{CCI}	α_{CCH}	α_{CCC}	γ_{CCCH}	γ_{CCCC}
$1^1\Sigma_g^+$	CAS(8,8)	6-31G**	1.056	1.212	1.384				
	SCF CI ^b	4-31G	1.065	1.219	1.374				
	MP2	6-31G**	1.063	1.226	1.375				
	MP2	aug-cc-pVDZ	1.074	1.239	1.383				
	exp ^c		1.061	1.210	1.371				
2^1B_g	CAS(8,8)	6-31G**	1.073	1.384	1.261	128.9	162.2		
2^1A_g	CAS(8,8)	6-31G**	1.075	1.342	1.307	128.2	169.6		
1^1B_g	CAS(8,8)	6-31G**	1.075	1.344	1.338	125.2	154.9		
$1^1\Delta_u$	CAS(8,8)	6-31G**	1.054	1.276	1.295				
	CAS(8,8)	4-31G	1.057	1.284	1.298	169.5	170.6		
	SCF CI ^b	4-31G	1.064	1.282	1.301	168.0	173.5		
1^1A_u	CAS(8,8)	6-31G**	1.071	1.304	1.295	131.9	163.6		
	CAS(8,8)	4-31G	1.066	1.303	1.292	135.8	165.7		
	SCF CI ^b	4-31G	1.082	1.300	1.295	135.7	165.2		
4^3A	CAS(8,8)	6-31G**	1.064	1.303	1.382	140.5	162.7	209.6	213.9
1^3B_g	CAS(8,8)	6-31G**	1.072	1.318	1.458	132.4	133.7		
1^3A_g	CAS(8,8)	6-31G**	1.068	1.299	1.460	137.5	139.0		
2^3A	CAS(8,8)	6-31G**	1.064	1.304	1.289	141.4	171.6	183.9	261.3
2^3B	CAS(8,8)	6-31G**	1.065	1.307	1.290	140.8	169.8	192.6	244.4
1^3A_u	CAS(8,8)	6-31G**	1.073	1.318	1.292	129.0	160.8		
	CAS(8,8)	4-31G	1.069	1.316	1.288	132.0	163.2		
	SCF CI ^b	4-31G	1.081	1.306	1.290	134.7	165.6		
1^3B_u	CAS(8,8)	6-31G**	1.068	1.308	1.291	136.7	168.6		
	CAS(8,8)	4-31G	1.063	1.310	1.286	137.9	170.7		
	SCF CI ^b	4-31G	1.064	1.290	1.291	176.0	174.8		

^a Bond lengths in Å, angles in degrees. r_{CCo} and r_{CCI} refer to the bond lengths of the outer and inner CC bonds, respectively. ^b From ref 9. ^c From ref 23.

the $1^1\Sigma_u^-$, $1^1\Delta_u$, $1^1\Sigma_g^-$, and $1^1\Delta_g$ states of the linear molecule) were considered. For vertical excitation (i.e., in $D_{\infty h}$ symmetry) these states are expected to lie energetically below any Rydberg states of the same symmetry. (This follows from the earlier discussion.) However, upon cis or trans bending of the molecule, the states derived from the valence $1\Sigma_g^-$ and $1\Delta_g$ states and from the Rydberg Π_g states are close in energy and of the same symmetries, and this opens up the possibility of valence/Rydberg mixing or “collapse” of the calculations onto the Rydberg states. Yet analysis of the CASSCF wave functions of the states in question shows that they retain their valence character even for the bent structures, perhaps due to the greater stabilization of the valence-like states upon distortion away from the linear structure. For this reason, we will not further consider the Rydberg states.

To account for dynamical electron correlation effects, in particular $\sigma-\pi$ correlation, CASPT2 calculations were carried out using the CAS(8,8) optimized geometries and using the CAS(8,8) wave functions as the reference functions. The Hamiltonian partitioning and the Fock operator used for the CASPT2 calculations are described in ref 14. Both the 6-31G** and ANO Gaussian-type orbital basis sets were used for the CASSCF and CASPT2 calculations. The former basis set is contracted to 3s2p1d and 2slp on the C and H atoms, respectively. The corresponding contractions in the ANO basis set are 4s3p2dlf and 3s2p1d. The CASSCF geometry optimizations and the CASPT2 single-point calculations were carried out using the MOLCAS software package.²¹ The CASSCF vibrational frequency calculations were performed using the Gaussian 98 package.²²

Results

Optimized Structures. Four of the states considered in the triplet manifold are predicted to exist as cis and trans isomers. Two of these are derived from the $1^3\Sigma_u^+$ and $1^3\Sigma_g^+$ states, and the other two are derived from the $1^3\Delta_u$ and $1^3\Delta_g$ states (one from each). The cis and trans optimized structures of the states

derived from the other components of the $1^3\Delta_u$ and $1^3\Delta_g$ states and from the $1^3\Sigma_u^-$ state are unstable to distortion to nonplanar C_2 symmetry structures. Convergence difficulties were encountered when attempting to optimize the distorted species derived from the $1^3\Sigma_g^-$ state, and we were forced to abandon these optimizations. In the singlet manifold, the $1^1\Delta_u$ state is predicted to remain linear, while the other states considered (those derived from $1^1\Sigma_u^-$, $1^1\Sigma_g^-$, and $1^1\Delta_g$) are all predicted to exist as cis and trans isomers.

The geometrical parameters obtained from the CAS(8,8)/6-31G** optimizations of the ground and excited states of diacetylene are summarized in Table 1. For the ground electronic state, the bond lengths of the terminal and interior CC bonds are predicted to be 1.21 and 1.38 Å, respectively, in good agreement with the corresponding experimental values of 1.21 and 1.37 Å.²³ For those states with cis and trans potential energy minima, the major structural difference between the two isomers is in the CCC angles, which tend to be larger (by up to 5.8°) in the cis isomer. Otherwise, the cis and trans isomers have very similar structures, with the obvious exception of the dihedral angles that distinguish the two. Accordingly, we will limit the detailed discussion of the structures to the trans species.

As was noted previously by Karpfen and Lischka, the CC bond lengths of the low-lying electronically excited states of diacetylene differ significantly from those of the ground state. In the excited singlet and triplet states dominated by the HOMO \rightarrow LUMO ($1\pi_g \rightarrow 2\pi_u^*$) excitations, the three CC bond lengths are predicted to be nearly equal (ranging from 1.28 to 1.32 Å) and significantly greater than in the electronic ground state. This is consistent with the bonding/antibonding characteristics of the MO's involved in the excitations and is indicative of these excited states having considerable cummulenic character.

The higher-lying 1^3B_g and 1^3A_g states are predicted to have terminal CC bond lengths near 1.30 Å and a central CC bond length near 1.46 Å, while the corresponding bond lengths in the 2^3A state are 1.30 and 1.38 Å. Again these bond lengths are consistent with the shape and nodal characteristics of the

TABLE 2: Calculated Vibrational Frequencies (cm⁻¹) for the Ground and Excited States of Diacetylene^a

	¹ Σ _g	¹ A _u	¹ Δ _u	¹ B _g	² A _g	² B _g	³ B _u	³ A _u	² 3B	² 3A	¹ 3A _g	¹ 3B _g	⁴ 3A
CCC, A, ip	221	275	275	289	207	254	172	254	281	304	280	291	256
CCC, S, op	221	291	275	288	235	276	168	263	231	240	252	275	154
CCC, A, op	646	611	573	707	431	460	455	610	452	471	770	836	469
CCC, S, ip	646	419	573	354	147	400	251	383	405	452	435	420	338
CCH, A, op	529		269										
CCH, S, ip	529	868	269	1009	1055	951	867	909	647	385	817	857	525
CCH, S, op	570	978	258	916	864	780	727	978	836	1275	768	896	841
CCH, A, ip	570	992	258	1110	1113	1042	1000	1050	901	883	970	1007	920
Mixed, ^b S		988		893	882	898	981	982	967	969	1059	1047	901
CCi, S	918		1008										
CCo, A	2152	1835	1971	1688	1736	1583	1851	1787	1846	1858	1824	1733	1841
Mixed, ^c S	2343	2201	2324	1908	2010	2294	2045	2087	2109	2089	1896	1777	1962
CH, S	3631	3419	3653	3363	3359	3391	3454	3395	3497	3500	3466	3416	3515
CH, A	3632	3423	3661	3365	3367	3396	3461	3398	3503	3508	3470	3419	3516

^a S and A denote symmetric and antisymmetric with respect to a rotation around the C₂ axis. ip and op denote in-plane and out-of-plane vibrations, respectively. ^b CCi, S + CCo, S + CCH, S, ip. ^c CCi, S + CCo, S.

MO's involved in the excitations. The last three states considered (¹B_g, ²A_g, and ²B_g) have terminal CC bond lengths ranging from 1.34 to 1.38 Å and an inner CC bond length ranging from 1.26 to 1.34 Å.

With the exception of the ¹Δ_u state, which is predicted to be linear, all excited states considered have highly bent CCH groups, with the CCH angles ranging from 125 to 141°. The CCC angles of the bent species range from 134 to 172°. The smallest CCC angles occur for the ¹3A_g and ¹3B_g states (139 and 134°, respectively); those for the other states are 155° or larger. Thus, the two states with the longest (~1.46 Å) central CC bond have the smallest CCC angles. The geometries of the ¹3A_g and ¹3B_g states are similar to that of the ground electronic state of butadiene, except for the presence of the four additional H atoms in the latter.

The nonplanar species have CCCC dihedral angles ranging from 209 to 261° and CCCH dihedral angles ranging from 184 to 210°. Examination of the potential energy curves shown in Figures 2 and 3 reveals that the states for which the energy increases with bending away from the linear structure either retain a linear geometry (¹Δ_u) or adopt a twisted structure (²3B, ²3A, ⁴3A).

The two lowest energy triplet and the two lowest energy excited singlet states of diacetylene were also considered by Karpfen and Lischka. Of these, there is good agreement between our structures and those of these authors for the A_u/A₂ states, but significant differences for the B_u/B₂ states. Although the KL study reports the ¹B_u state (and its ¹B₂ isomeric counterpart) of diacetylene to be weakly bent, with CCH and CCC angles of 174 and 168°, respectively, we find this state to be linear, corresponding to one component of the ¹Δ_u state. A larger discrepancy exists between the two sets of theoretical results for the ¹3B_u state, which we find to be strongly bent (CCC and CCH angles of 168.6 and 136.7°, respectively), but which Karpfen and Lischka report as being close to linear, with CCC and CCH angles of 174.8 and 176.0°, respectively.

We have also optimized the structures of the excited states in question using the 4-31G basis set, which was used by Karpfen and Lischka. The CAS(8,8)/4-31G calculations predict the ¹B_u state to have a bent structure, as reported by Karpfen and Lischka, but in contrast to our CAS(8,8)/6-31G** calculations. Thus, it appears that the use of the small 4-31G basis set incorrectly leads to a bent structure in this case. However, for the ¹3B_u state, the CAS(8,8)/4-31G calculations give a structure similar to that obtained from the CAS(8,8)/6-31G** optimization. This leads us to conclude that for the ¹3B_u state, either differences in the treatment of electron correlation effects or in

how the optimizations were carried out are responsible for the more highly bent structure reported here than in the study of Karpfen and Lischka. Specifically, we note that the MCSCF and CI approaches used by Karpfen and Lischka do not provide as balanced a description of the π-electron correlation effects as does the CAS(8,8) approach employed in this work. Also, while we used analytical gradients, Karpfen and Lischka optimized their structures through grid searches, a procedure which sometimes fails to correctly locate minimum energy structures.

Vibrational Frequencies. Table 2 reports for the low-lying electronic states of diacetylene the normal-mode frequencies calculated at the CAS(8,8)/6-31G** level of theory. In those cases that there are both cis and trans isomers, only the frequencies of the trans isomer are reported, as those for the cis isomer are similar. The different modes are labeled as symmetric or antisymmetric with respect to rotation about the C₂ axis as well as in-plane or out-of-plane with respect to the plane perpendicular to that axis. For the non-twisted species the reflection plane contains the C atoms. For the states with twisted structures, this plane is obviously not a true symmetry plane. For the ground state, the calculated vibrational frequencies, after scaling by a factor of 0.92 to account for anharmonicity effects and incomplete treatment of electron correlation, are in good agreement with the experimental values²⁴ of the frequencies. However, it is likely that use of more flexible basis sets and inclusion of dynamical correlation effects will be necessary to reliably predict the vibrational frequencies of the electronically excited states. We plan to consider these factors in a future study. Nonetheless, for examining the qualitative trends in the frequencies the CAS(8,8)/6-31G** results should suffice.

As expected, the trends in the vibrational frequencies correlate well with those in the geometrical parameters. This is seen, for example, in Figure 4 which plots the calculated frequency of the asymmetric CC stretch as a function of the length of the outer CC bonds. The trends in the frequencies of the symmetric CC stretch modes are less readily apparent because these depend on the lengths of both the central and outer CC bonds. The frequencies of the two high-frequency CC stretch modes are also appreciably lower for the excited states than for the ground state (the exception being the ¹Δ_u state for which the highest frequency CC stretch vibration has a frequency nearly the same as that in the ground state).

With the exception of the ¹Δ_u state, the CH stretching frequencies are appreciably lower for the excited states than for the ¹Σ_g⁺ ground state, with the frequency reduction being less for the twisted than for the planar-distorted species. This

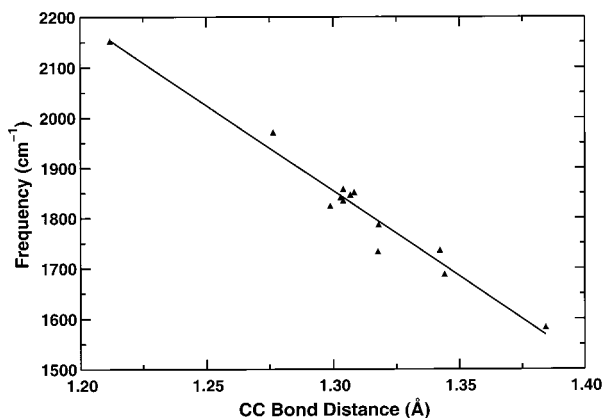


Figure 4. Correlation between the frequency of the asymmetric CC stretch mode and the length of the outer CC bonds for the various electronic states of diacetylene. The results displayed are from CAS-(8,8)/6-31G** calculations.

is due to the fact that, although nonplanar, these structures are almost linear. With the exception of the $1^1\Delta_u$ and 2^3A states, the CCH bending frequencies are significantly larger (by up to 563 cm^{-1}) in the excited states than in the ground state. For the $1^1\Delta_u$ state the frequencies of the two CCH bending modes are $260\text{--}312\text{ cm}^{-1}$ lower than in the ground state, and for the 2^3A state the frequency of one of the CCH bending vibrations is 144 cm^{-1} lower than that in the electronic ground state. In general, the CCC bend vibrations occur at lower frequencies in the excited states than in the ground state, the exceptions occurring for the 1^1B_g , 1^3A_g , and 1^3B_g states. For each of these states, one of the CCC bending vibrations occurs at a higher frequency than in the ground state.

Dominant Configurations. Tables 3 and 4 report the dominant configurations in the CASSCF wave function for each of the states considered. Results are reported for both vertical excitation (i.e., at the geometry for the ground electronic state) as well as for the optimized structures of the excited states. The results for vertical excitation are considered first.

The low-lying $3^3\Sigma_u^+$, $3^3\Delta_u$, $3^3\Sigma_u^-$, $1^1\Sigma_u^-$, and $1^1\Delta_u$ states are all dominated by two configurations, involving HOMO \rightarrow LUMO excitations. These enter the wave function with equal weights, with a combined weight ranging from 82.8 to 87.6%. Not surprisingly, the higher-lying $3^3\Sigma_g^+$, $3^3\Delta_g$, $3^3\Sigma_g^-$, $1^1\Delta_g$, and $1^1\Sigma_g^-$ excited states all display more extensive configurational mixing with the combined weight of the two dominant (HOMO-1 \rightarrow LUMO) configurations ranging from 66.6 to 76.8%. With the exception of the $1^1\Delta_g$ state, the next most important class of configurations in this group of states is of the type HOMO \rightarrow LUMO + 1. In the case of the $1^1\Delta_g$ state, it is a double excitation of the form (HOMO) $^2 \rightarrow$ (LUMO) 2 .

We now consider the dominant configurations in the wave functions associated with the optimized structures of the excited states. In those cases that there are cis and trans isomers, only the trans isomers are considered, as the configuration mixing is similar in the cis isomer. The triplet states are considered first. The lowest-lying triplet state, 1^3B_u ($3^3\Sigma_u^+$), is dominated by the $a_g \rightarrow b_u$ ($1\pi_{gy} \rightarrow 2\pi_{uy}^*$) excitation, while the next lowest triplet state, 1^3A_u ($3^3\Delta_u$), is dominated by the $b_g \rightarrow b_u$ ($1\pi_{gx} \rightarrow 2\pi_{uy}^*$) excitation. (In specifying the term symbols, the symmetries of the corresponding states for the $D_{\infty h}$ structures are indicated in parentheses. The linear molecule is assumed to be aligned along the z axis and the bending is assumed to occur in the yz plane.) Thus, both of these states are dominated by configurations involving excitation into the in-plane component of the $1\pi_u^*$ orbital.

TABLE 3: Dominant Configurations in the CAS(8,8)/6-31G Wavefunctions of the Vertically Excited, Low-lying Electronic States of Diacetylene^a**

$D_{\infty h}$	$1\pi_{ux}$	$1\pi_{uy}$	$1\pi_{gx}$	$1\pi_{gy}$	$2\pi_{ux}^*$	$2\pi_{uy}^*$	$2\pi_{gx}^*$	$2\pi_{gy}^*$	%
$1^1\Sigma_g^+$	2	2	2	2	0	0	0	0	87.7
$1^1\Delta_g$	1	2	2	2	1	0	0	0	38.2
	2	1	2	2	0	1	0	0	38.2
	2	2	0	2	2	0	0	0	5.0
	2	2	2	0	0	2	0	0	5.0
	2	1	2	2	1	0	0	0	38.2
	1	2	2	2	0	1	0	0	38.2
$1^1\Sigma_g^-$	2	1	2	2	1	0	0	0	38.6
	1	2	2	2	0	1	0	0	38.6
$1^1\Delta_u$	2	2	1	2	0	1	0	0	44.6
	2	2	2	1	1	0	0	0	44.6
	2	2	1	2	1	0	0	0	44.6
	2	2	2	1	0	1	0	0	44.6
$1^1\Sigma_u^-$	2	2	1	2	0	1	0	0	44.0
	2	2	2	1	1	0	0	0	44.0
$1^1\Sigma_g^-$	2	1	2	2	1	0	0	0	38.4
	1	2	2	2	0	1	0	0	38.4
$1^3\Delta_g$	1	2	2	2	1	0	0	0	35.8
	2	1	2	2	0	1	0	0	35.8
	2	2	1	2	0	0	1	0	8.5
	2	2	2	1	0	0	0	1	8.5
	2	1	2	2	1	0	0	0	35.8
	1	2	2	2	0	1	0	0	35.8
	2	2	2	1	0	0	1	0	8.5
	2	2	1	2	0	0	0	1	8.5
$1^3\Sigma_g^+$	1	2	2	2	1	0	0	0	33.3
	2	1	2	2	0	1	0	0	33.3
	2	2	1	2	0	0	1	0	11.4
	2	2	2	1	0	0	0	1	11.4
$1^3\Sigma_u^-$	2	2	1	2	0	1	0	0	43.8
	2	2	2	1	1	0	0	0	43.8
$1^3\Delta_u$	2	2	1	2	0	1	0	0	42.8
	2	2	2	1	1	0	0	0	42.8
	2	2	1	2	1	0	0	0	42.8
	2	2	2	1	0	1	0	0	42.8
$1^3\Sigma_u^+$	2	2	1	2	1	0	0	0	41.4
	2	2	2	1	0	1	0	0	41.4

^a Calculated at the CAS(8,8)/6-31G** optimized ground state geometry. Only configurations with weights greater than 5% are listed. In the case of degenerate states, the weights for both components are reported.

The configuration mixing in the 2^3B ($3^3\Delta_u$), 2^3A ($3^3\Sigma_u^-$), and 4^3A ($3^3\Delta_g$) states is quite similar to that in the linear states from which they are derived. In contrast, the wave functions for the 1^3A_g ($3^3\Sigma_g^+$) and 1^3B_g ($3^3\Delta_g$) states contain configurations with sizable weights (33.6 and 39.1%) that were relatively unimportant (<11.5%) in their linear counterparts.

The wave function of the lowest energy excited singlet state, 1^1A_u , is dominated, as expected, by the $b_g \rightarrow b_u$ ($1\pi_{gx} \rightarrow 2\pi_{uy}^*$) configuration. The wave function of the next higher energy singlet state, $1^1\Delta_u$, is dominated by two configurations of equal weight (again derived from HOMO \rightarrow LUMO excitations.) The next three singlet states all have appreciably doubly-excited character. The 2^1A_g and 1^1B_g states, based on the dominant configurations in their wave functions, can be viewed as being derived from the $1^1\Delta_g$ state. On the other hand, the 2^1B_g state, which we had expected to be derived from $1^1\Sigma_g^-$, is predominantly doubly excited in nature, with the most important configurations being $(1\pi_{gx})^2 \rightarrow 2\pi_{uy}^*2\pi_{ux}^*$ and $1\pi_{gx}1\pi_{gy} \rightarrow (2\pi_{uy}^*)^2$. It is possible that this state actually corresponds to the 3^1B_g state, with the 2^1B_g state having been inadvertently missed in the CASSCF calculations. Attempts to extract another 1^1B_g root from the CASSCF calculations proved unsuccessful.

Excitation Energies. Vertical Excitation. Table 5 reports the vertical excitation energies of diacetylene calculated at the CAS-(8,8)/6-31G**, CAS(8,8)/ANO, CASPT2/6-31G**, and CASPT2/ANO levels of theory. These results were obtained using the

TABLE 4: Dominant Configurations in the CAS(8,8)/6-31G Wavefunctions of the Low-Lying Electronic States of Diacetylene^a**

$D_{\infty h}$	$1\pi_{ux}$	$1\pi_{uy}$	$1\pi_{gx}$	$1\pi_{gy}$	$2\pi_{ux}^*$	$2\pi_{uy}^*$	$2\pi_{gx}^*$	$2\pi_{gy}^*$	
C_{2h}	$1a_u$	$1b_u$	$1b_g$	$1a_g$	$2a_u$	$2b_u$	$2b_g$	$2a_g$	
C_2	1a	1b	2b	2a	3a	3b	4b	4a	%
$1^1\Sigma_g^+$	2	2	2	2	0	0	0	0	87.7
2^1B_g	2	2	0	2	1	1	0	0	44.1
	2	2	1	1	0	2	0	0	25.5
	1	2	2	2	0	1	0	0	12.1
1^1B_g	1	2	2	2	0	1	0	0	50.6
	2	2	1	1	0	2	0	0	22.6
2^1A_g	2	1	2	2	0	1	0	0	31.1
	2	2	2	0	0	2	0	0	26.1
	2	2	1	1	1	1	0	0	11.8
	2	2	2	1	0	0	0	1	5.5
$1^1\Delta_u$	2	2	1	2	0	1	0	0	44.4
	2	2	2	1	1	0	0	0	44.4
	2	2	1	2	1	0	0	0	44.4
	2	2	2	1	0	1	0	0	44.4
1^1A_u	2	2	1	2	0	1	0	0	87.7
4^3A	1	2	2	2	1	0	0	0	33.8
	2	1	2	2	0	1	0	0	29.9
	2	2	2	1	0	0	0	1	6.8
	2	2	1	2	0	0	1	0	6.3
1^3B_g	2	2	1	2	0	0	0	1	39.2
	1	2	2	2	0	1	0	0	39.1
1^3A_g	2	1	2	2	0	1	0	0	43.9
	2	2	2	1	0	0	0	1	33.6
2^3A	2	2	2	1	1	0	0	0	42.5
	2	2	1	2	0	1	0	0	41.5
2^3B	2	2	1	2	1	0	0	0	41.3
	2	2	2	1	0	1	0	0	40.7
1^3A_u	2	2	1	2	0	1	0	0	79.1
1^3B_u	2	2	2	1	0	1	0	0	69.9
	2	2	1	2	1	0	0	0	10.9

^a Calculated at the CAS(8,8)/6-31G** optimized geometry for each excited state. Only configurations with weights greater than 5% are listed. In the case of degenerate states, the weights for both components are reported.

CAS(8,8)/6-31G** optimized geometry of the ground state. Where available, experimental values for the vertical excitation energies have been included for comparison. In discussing the theoretical results we will focus on those obtained at the highest level of theory, i.e., CASPT2/ANO.

The CASPT2/ANO calculations give vertical excitation energies of 3.69, 4.45, and 5.01 eV for the $1^3\Sigma_u^+$, $1^3\Delta_u$, and $1^3\Sigma_u^-$ states, respectively, and 5.73, 6.58, and 7.19 eV for the $1^3\Sigma_g^+$, $1^3\Delta_g$, and $1^3\Sigma_g^-$ states, respectively. On the basis of electron energy loss measurements,¹⁹ it has been concluded that the vertical excitation energies of the two lowest energy triplet states are 3.2 ± 0.5 and 4.2 ± 0.2 eV. The electron energy loss spectra obtained at low residual electron energies also display features peaked near 5.2 and 7.1 eV that may correspond to excitation of the $1^3\Sigma_u^-$ and $1^3\Sigma_g^-$ states.

The CASPT2/ANO calculations give vertical excitation energies of 5.02, 5.32, 7.34, and 7.33 eV for formation of the $1^1\Sigma_u^-$, $1^1\Delta_u$, $1^1\Sigma_g^-$, and $1^1\Delta_g$ states, respectively. Experimentally, the vertical transition to form the $1^1\Delta_u$ state has been found to occur at 5.32 eV.¹⁹ The vertical transition for forming the $1^1\Sigma_u^-$ state has been reported to occur at 4.81 eV.^{19,25} We note also that the electron energy loss spectra display transitions with maxima near 7.1 and 7.5 eV, which, based on their dependence on the residual energy, could correspond to the $1^1\Sigma_g^-$, and $1^1\Delta_g$ states. Thus, although there are uncertainties in assigning many of the features in the observed spectra, for those states for which the assignments are reasonably secure, the vertical excitation energies predicted by the CASPT2/ANO procedure are in good agreement with experiment.

Adiabatic Excitation. Table 6 reports the calculated and experimental adiabatic excitation energies of diacetylene. In those cases that there are cis and trans isomeric pairs, the energies of the isomers are found to agree to within 0.03 eV, and, for this reason, only the results for the trans isomer are discussed. As for the vertical excitation energies, theoretical results are reported at the CAS(8,8)/6-31G**, CAS(8,8)/ANO, CASPT2/6-31G**, and CASPT2/ANO levels of theory, using CAS(8,8)/6-31G** optimized geometries. Table 6 also reports adiabatic excitation energies calculated at the CAS(8,8)/4-31G level of theory. These results have been included to facilitate comparison with the results of Karpfen and Lischka who employed the 4-31G basis set in most of their calculations. The excitation energies obtained from the CAS(8,8)/6-31G** and CAS(8,8)/ANO calculations agree to within 0.1 eV. However, those from the CAS(8,8)/4-31G calculations are up to 0.3 eV higher in energy, reflecting the inadequacy of the 4-31G basis set for describing the excited states.

As noted above, Karpfen and Lischka reported theoretical results for the 1^3B_u , 1^1B_u , 1^3A_u , and 1^1A_u states of diacetylene. For the 1^3A_u state, the CAS(8,8)/4-31G calculations give an adiabatic excitation energy very close to the CI/4-31G result of Karpfen and Lischka. On the other hand, there are sizable differences in the two sets of excitation energies in the case of the other states. Specifically, the CI calculations place the 1^3B_u state about 0.3 eV higher in energy and the 1^1B_u and 1^1A_u states 0.4 eV lower in energy (relative to the ground state) than do our CAS(8,8)/4-31G calculations. However, the discrepancy may be due to the aforementioned differences in the geometries as determined by the CAS(8,8)/4-31G and CI/4-31G calculations.

For the low-lying states, the CASPT2 excitation energies obtained using the 6-31G** and ANO basis sets are fairly close, agreeing to within 0.2 eV. However, for the high-lying states (in both the singlet and triplet manifolds), the CASPT2 calculations with the more flexible ANO basis set give excitation energies 0.3–0.5 eV lower in energy than the corresponding results with the 6-31G** basis set. Hereafter, we focus on the results of the CASPT2/ANO calculations as they should be the most reliable.

The CASPT2/ANO calculations give adiabatic excitation energies of 2.97 and 3.43 eV for the 3B_u and 3A_u states, respectively. These results are in fairly good agreement with the corresponding experimental values of 2.7 and 3.22 eV.¹⁹ Similarly, fairly good agreement is found between theory and experiment for the adiabatic excitation energies of the lowest two singlet states, with the theoretical results being 4.07 (1^1A_u) and 5.15 eV ($1^1\Delta_u$), as compared to the experimental values of 4.33 and 5.06 eV.^{19,25,26}

The CASPT2/ANO calculations place the origins of the higher-lying triplet states at 3.81 (3B), 4.25 (3A), 5.02 (3A_g), 5.60 (3B_g), and 5.85 eV (3A), and the higher-lying singlet states at 5.65 (1^1A_g), 5.98 (1^1B_g), and 6.93 eV (1^1B_g). Even though the electron energy loss spectra display considerable structure throughout the 3.5–7 eV region, assigning this structure is difficult because of overlapping states and the large geometrical changes accompanying electronic excitation (resulting in broad transitions.) The problem is particularly severe for energies above 5 eV for which the calculations predict overlapping triplet and dipole-forbidden singlet states.

In the triplet manifold, the differences between the calculated vertical and adiabatic excitation energies range from 0.65 to 1.02 eV, with the energy lowerings being greatest for the $1^3\Delta_u \rightarrow 1^3A_u$ and $1^3\Delta_g \rightarrow 1^3B_g$ geometry distortions. It should be

TABLE 5: Vertical Excitation Energies (eV) of Diacetylene Relative to the $1^1\Sigma_g^+$ Ground State

state	CAS(8,8)/6-31G**	CAS(8,8)/ANO	CASPT2/6-31G**	CASPT2/ANO	exp ^a
$1^1\Sigma_g^-$	8.53	8.46	7.61	7.34	7.5
$1^1\Delta_g$	8.76	8.69	7.73	7.33	7.1
$1^1\Delta_u$	6.79	6.69	5.75	5.32	5.32
$1^1\Sigma_u^-$	6.36	6.30	5.44	5.02	4.81 ^b
$1^3\Sigma_g^-$	8.53	8.48	7.56	7.19	7.1
$1^3\Delta_g$	7.74	7.70	6.96	6.58	
$1^3\Sigma_g^+$	6.79	6.79	6.00	5.73	
$1^3\Sigma_u^-$	6.32	6.26	5.34	5.01	5.2
$1^3\Delta_u$	5.55	5.51	4.75	4.45	4.3 ± 0.2
$1^3\Sigma_u^+$	4.67	4.67	3.86	3.69	3.2 ± 0.5

^a Taken from ref 19 unless otherwise noted. ^b From ref 25.

TABLE 6: Adiabatic Excitation Energies (eV) of Diacetylene Relative to the $1^1\Sigma_g^+$ Ground State

symmetry	state	CI/4-31G ^a	CAS(8,8)/4-31G	CAS(8,8)/6-31G**	CAS(8,8)/ANO	CASPT2/6-31G**	CASPT2/ANO	exp
C_{2h}	2^1B_g			8.10	8.11	7.23	6.93	
C_{2h}	1^1B_g			6.99	7.07	6.07	5.98	
C_{2h}	2^1A_g			6.46	6.56	5.68	5.65	
D_{2h}	$1^1\Delta_u$	6.05	6.44	6.21	6.13	5.17	5.15	5.06 ^b
C_{2h}	1^1A_u	5.30	5.56	5.20	5.19	4.27	4.07	4.33 ^c
C_2	4^3A			7.15	7.21	6.34	5.85	
C_{2h}	1^3B_g			6.33	6.40	5.66	5.60	
C_{2h}	1^3A_g			5.40	5.51	4.95	5.02	
C_2	2^3A			5.58	5.60	4.54	4.25	
C_2	2^3B			4.69	4.73	3.91	3.81	
C_{2h}	1^3A_u	4.41	4.48	4.20	4.25	3.49	3.43	3.22 ^d
C_{2h}	1^3B_u	3.93	3.58	3.51	3.60	2.93	2.97	2.7 ^d
C_{2v}	1^1A_2			5.22	5.19	4.31	4.09	
C_{2v}	1^3A_2			4.23	4.26	3.54	3.47	
C_{2v}	1^3B_2			3.52	3.60	2.95	2.99	

^a From ref 9. ^b From ref 25. ^c From ref 26. ^d From ref 19.

TABLE 7: Vertical Excitation Energies (eV) of Diacetylene Relative to the Cis (1^3B_u) and Trans (1^3B_2) Potential Energy Minima

symmetry		CAS(8,8)/ANO	CASPT2/ANO
C_{2h}	2^3A_u	2.61	2.12
	1^1B_u	2.89	2.02
	1^1A_u	1.61	1.15
	2^3B_u	1.44	1.10
C_{2v}	1^3A_u	0.70	0.50
	2^3A_2	2.59	2.10
	1^1B_2	2.89	2.02
	1^1A_2	1.62	1.16
	2^3B_2	1.44	1.10
	1^3A_2	0.71	0.52

kept in mind that not all of the relaxation energy is associated with the distortions away from the linear structure, since the CC and CH bond lengths also change upon electronic excitation. In the singlet manifold, the spread in relaxation energies is even greater, ranging from 0.17 eV for the $1^1\Delta_u$ state (which retains its linear structure) to 1.68 eV for the 2^1A_g state. The large relaxation energy in the latter case may be the result of the sizable increase in the doubly-excited character in the wave function, accompanying the distortion from the linear to the bent structure.

Table 7 reports vertical excitation energies relative to the lowest triplet state of diacetylene in both the cis and trans configurations. These energies are relevant for designing experiments to observe higher-lying triplet states via direct triplet-triplet absorption. The triplet-triplet excitation energies calculated for the cis and trans structures agree to within 0.02 eV. In C_{2v} symmetry, two of the three HOMO \rightarrow LUMO transitions, namely $1^3B_2 \rightarrow 1^3A_2$ and $1^3B_2 \rightarrow 2^3A_2$ are dipole-allowed. These are predicted to fall at 0.52 and 2.10 eV. In contrast, in C_{2h} symmetry, none of the HOMO \rightarrow LUMO transitions are dipole allowed.

Conclusions

The CASSCF and CASPT2 methods have been used to characterize the low-lying electronically excited valence states of diacetylene. In the triplet manifold, the geometries of seven low-lying states were optimized, four of which are predicted to exist as cis/trans isomeric pairs and three of which are predicted to be distorted nonplanar. In the singlet manifold, the $1^1\Delta_u$ state retains a linear structure, whereas the other states considered are predicted to exist as cis/trans isomeric pairs. In those cases that the experimental excitation energies (and state assignments) are known, there is good agreement between theory and experiment. Tentative assignments are made for some of the higher lying features observed in the electronic absorption and electron energy loss spectra of diacetylene. Vibrational frequencies, calculated in the harmonic approximation, have been reported for the ground and excited states.

Although not discussed in the main body of the paper, we have also optimized the transition states for cis/trans isomerization of the two lowest triplet states.²⁷ The calculated barrier heights for the $^3B_u \rightarrow ^3B_2$ and $^3A_u \rightarrow ^3A_2$ isomerizations are predicted to be 3.1 and 3.6 kcal/mol, respectively. These results indicate that for sufficiently cold diacetylene molecules, the interconversion between the cis and trans isomers should be quite slow, making it possible to spectroscopically characterize the individual isomeric species.

Acknowledgment. This research was carried out with support from NSF (F.V. and K.D.J.) and Pacific Northwest Laboratories (P.B.). We thank Prof. Tim Zwier for interesting discussions about the excited states of diacetylene. Some of the calculations were carried out on computers in the University of Pittsburgh's Center for Molecular and Materials Simulations and which were funded by NSF and IBM.

References and Notes

- (1) Yung, Y. L.; Allen, M.; Pinto, J. P. *Astrophys. J., Suppl. Ser.* **1984**, *55*, 465.
- (2) Sagan, C.; Thompson, W. R. *Icarus* **1984**, *59*, 1233.
- (3) Coustenis, A.; Bezzard, B.; Gautier, D.; Marten, A.; Samuelson, R. *Icarus* **1991**, *89*, 152.
- (4) Atreya, S. K.; Sandel, B. R.; Romani, P. N. In *Uranus*; Bergstrahl, J. T., Ed.; University of Arizona: Tucson, 1990.
- (5) Bandy, R. E.; Lakshminarayan, C.; Frost, R. K.; Zwier, T. S. *J. Chem. Phys.* **1993**, *98*, 5362.
- (6) Frost, R. K.; Zavarin, G. S.; Zwier, T. S. *J. Phys. Chem.* **1995**, *99*, 9408.
- (7) Frost, R. K.; Arrington, C. A.; Ramos, C.; Zwier, T. S. *J. Am. Chem. Soc.* **1996**, *118*, 4451.
- (8) Arrington, C. A.; Ramos, C.; Robinson, A. D.; Zwier, T. S. *J. Phys. Chem. A* **1998**, *102*, 3315.
- (9) Karpfen, A.; Lischka, H. *Chem. Phys.* **1986**, *102*, 91.
- (10) Roos, B. O. *Int. J. Quantum Chem.* **1980**, *S14*, 175.
- (11) Roos, B. O.; Taylor, P. R.; Siegbahn, P. E. M. *Chem. Phys.* **1980**, *48*, 157.
- (12) Roos, B. O. In *Advances in Chemical Physics; Ab Initio Methods in Quantum Chemistry-II*; Lawley, K. P., Ed.; John Wiley & Sons Ltd.: Chichester, England, 1987.
- (13) Andersson, K.; Malmqvist, P.-Å.; Roos, B. O.; Sadlej, A. J.; Wolinski, K. *J. Phys. Chem.* **1990**, *94*, 5483.
- (14) Andersson, K.; Malmqvist, P.-Å.; Roos, B. O. *J. Chem. Phys.* **1992**, *96*, 1218.
- (15) Andersson, K.; Roos, B. O. In *Modern Electron Structure Theory*; Yarkony, R., Ed.; World Scientific Publishing: New York, 1994; Vol. 1.
- (16) Hehre, W. J.; Ditchfield, R.; Pople, J. A. *J. Chem. Phys.* **1972**, *56*, 2257.
- (17) Hariharan, P. C.; Pople, J. A. *Theor. Chim. Acta* **1973**, *28*, 213.
- (18) Dill, J. D.; Pople, J. A. *J. Chem. Phys.* **1975**, *94*, 69.
- (19) Allan, M. J. *Chem. Phys.* **1984**, *80*, 6020.
- (20) Widmark, P.-O.; Malmqvist, P.-Å.; Roos, B. O. *Theor. Chim. Acta* **1990**, *77*, 291.
- (21) Andersson, K.; Blomberg, M. R. A.; Fülscher, M. P.; Karlström, G.; Lindh, R.; Malmqvist, P.-Å.; Neogrády, P.; Olsen, J.; Roos, B. O.; Sadlej, A. J.; Schütz, M.; Seijo, L.; Serrano-Andrés, L.; Siegbahn, P. E. M.; Widmark, P.-O. *MOLCAS*, Version 4; Lund University, Sweden, 1997.
- (22) Frisch, M. J.; Trucks, G. W.; Schlegel, H. B.; Scuseria, G. E.; Robb, M. A.; Cheeseman, J. R.; Zakrzewski, V. G.; Montgomery, J. A., Jr.; Stratmann, R. E.; Burant, J. C.; Dapprich, S.; Millam, J. M.; Daniels, A. D.; Kudin, K. N.; Strain, M. C.; Farkas, O.; Tomasi, J.; Barone, V.; Cossi, M.; Cammi, R.; Mennucci, B.; Pomelli, C.; Adamo, C.; Clifford, S.; Ochterski, J.; Petersson, G. A.; Ayala, P. Y.; Cui, Q.; Morokuma, K.; Malick, D. K.; Rabuck, A. D.; Raghavachari, K.; Foresman, J. B.; Cioslowski, J.; Ortiz, J. V.; Stefanov, B. B.; Liu, G.; Liashenko, A.; Piskorz, P.; Komaromi, I.; Gomperts, R.; Martin, R. L.; Fox, D. J.; Keith, T.; Al-Laham, M. A.; Peng, C. Y.; Nanayakkara, A.; Gonzalez, C.; Challacombe, M.; Gill, P. M. W.; Johnson, B. G.; Chen, W.; Wong, M. W.; Andres, J. L.; Head-Gordon, M.; Replogle, E. S.; Pople, J. A. *Gaussian 98*, Revision A.7; Gaussian, Inc.: Pittsburgh, PA, 1998.
- (23) Tay, R.; Metha, G. F.; Shanks, F.; McNaughton, D. *Struct. Chem.* **1995**, *6*, 47.
- (24) Owen, N. L.; Smith, C. H.; Williams, G. A. *J. Mol. Struct.* **1987**, *161*, 33.
- (25) Haink, H.-J.; Jungen, M. *Chem. Phys. Lett.* **1979**, *61*, 319.
- (26) Hardwick, J. L.; Ramsay, D. A. *Chem. Phys. Lett.* **1977**, *48*, 399.
- (27) Vila, F.; Jordan, K. D. Unpublished results.